

Supplemental Information

Optimizing high-temperature energy storage capability enabled by regulating interchain spacing with tailored pendant group in self- crosslinkable polyetherimide

Huilei Jiang^a, Lixin Xu^{a,b*}, Huijian Ye^{a,b*}

^a College of Materials Science and Engineering, Zhejiang University of Technology, Hangzhou 310014, China

^b Zhejiang Key Laboratory of Advanced Polymer Materials Modification and Application Technology, Zhejiang University of Technology, Hangzhou 310014, China

* Corresponding author, E-mail: huy19@zjut.edu.cn (H. Ye), gcsxlx@zjut.edu.cn (L. Xu)

Characterization of PEQDA monomers and PEQDA-PAA

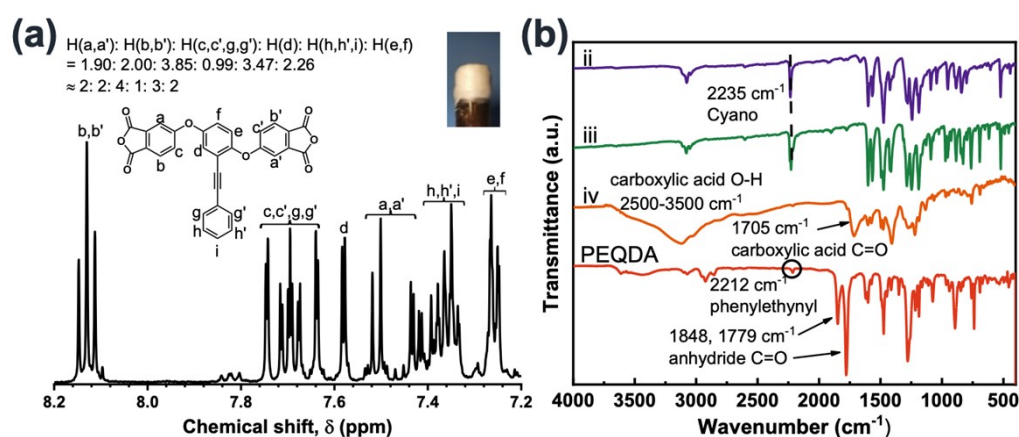


Figure S1. (a) ^1H NMR spectra and (b) FTIR results of PEQDA monomer

The structure of PEQDA monomer is analyzed by ^1H -NMR and FTIR, as shown in

Figure S1, to prove the successful synthesis of PEQDA monomer. Figure S1a shows the optical image and ^1H NMR spectra of the PEQDA monomer, which is a pale-yellow powder. The peak between 7.31-7.41 ppm corresponds to hydrogen at three positions on the benzene ring of the PEQDA suspension arm. The peaks at 7.56-7.59 ppm and 7.23-7.28 ppm both belong to the three types of hydrogen on the benzene ring adjacent to the alkyne group in the main chain. Peaks between 8.10-8.16 ppm and 7.42-7.53 ppm belong to the four types of hydrogen on the benzene ring adjacent to the imide ring. It is found that the ratio of the areas of different absorption peaks is approximately equal to the ratio of the number of hydrogen atoms, which proved the successful synthesis of the PEQDA monomer. Furthermore, after the reaction, the b, b' peaks shifted from 7.80-7.83 ppm to 8.10-8.16 ppm, and the purity of PEQDA could be calculated to be 90.91%. The FTIR spectrum of PEQDA monomer in Figure S1b shows a $\text{C}\equiv\text{C}$ stretching vibration peak at 2212 cm^{-1} , and antisymmetric stretching vibration and symmetric stretching vibration peaks of $\text{C}=\text{O}$ in the imide ring at 1848 cm^{-1} and 1778 cm^{-1} respectively. The disappearance of the OH absorption peak and the change of the $\text{C}=\text{O}$ absorption peak in the carboxylic acid at $2500\text{-}3500\text{ cm}^{-1}$ proved that the carboxylic acid successfully dehydrated to form the imide ring. ^1H NMR and FTIR results confirmed the synthesis of PEQDA monomer.

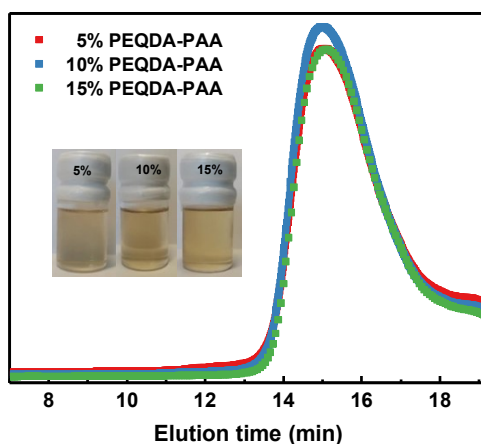


Figure S2. GPC curves of PEQDA-PAA samples.

Table S1. The molar ratio of monomers and the molecular weight of the PEQDA-PAA oligomers.

Sample	4,4'-ODA	BPADA	EBPA	$\bar{M}_{n,PS}$ (kD)	$\bar{M}_{w,PS}$ (kD)	PDI
5% PEQDA-PAA	50	49.4	2.6	4.4	9.8	2.2
10% PEQDA-PAA	50	46.8	5.2	4.7	10.1	2.1
15% PEQDA-PAA	50	44.2	7.8	4.4	9.4	2.1

GPC analyses are performed on a series of oligomers (PEQDA-PAA) to assess the number average molecular weights (M_n), the weight average molecular weights (M_w), and polydispersity index ($PDI = M_w/M_n$) with the results presents in Table S1. The molecular weight variation of oligomers is irregular with the increase of crosslinkable dianhydride ratio. In addition, the PDI of PEQDA-PAA is relatively narrow, $PDI \approx 2.1$, which is of great significance for the improvement of polymer properties.

Characterization and properties of crosslinking films

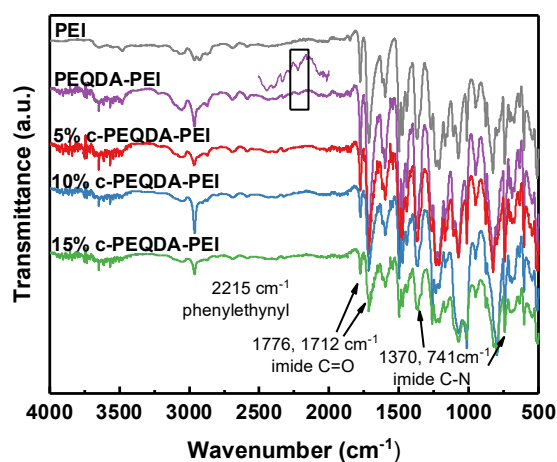


Figure S3. FT-IR curves of the c-PEQDA-PEI films.

The chemical structure of polyetherimide films before and after crosslinking was characterized by FT-IR spectroscopy, as shown in Figure S3. All the crosslinking films with different crosslinkable dianhydride ratio exhibited the similar absorptions. The characteristic peaks at 1776 and 1712 cm⁻¹ represent the symmetric and asymmetric stretching vibrations of C=O bonds in the imide group, respectively. The absorption bands at around 1370 and 741 cm⁻¹ assigned to the stretching and bending vibration of imide C-N are also detected. In particular, after crosslinking, it's clearly found that the absorption peak at 2215 cm⁻¹ is disappeared, belongs to phenylethynyl C≡C, indicating that the crosslinking reaction of C≡C groups is carried out.

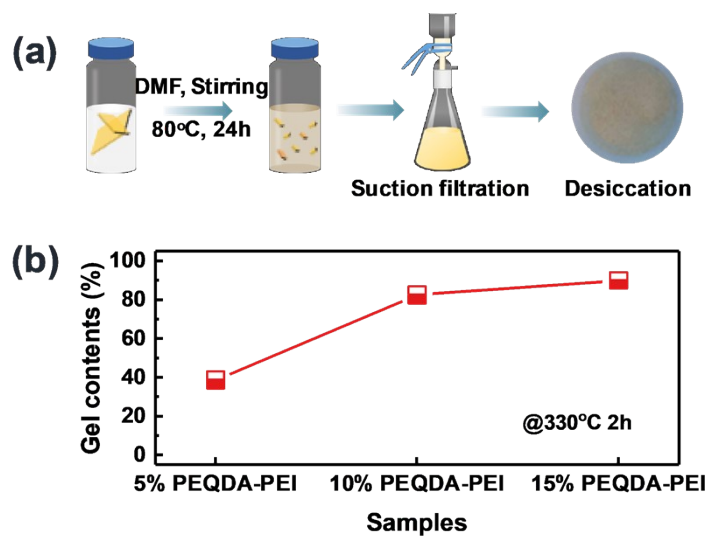


Figure S4. (a) Schematic diagram of test of gel content, (b) gel content of c-PEQDA-PEI films.

To study the relationship between gel content and PEQDA content, gel content of films was tested, as shown in Figure S4. Under the same heat treatment process, the gel content and the content of crosslinkable dianhydride PEQDA shows the same trend. When the heat treatment temperature is 330 °C and the heat treatment time is 2 h, the gel content of 5%, 10% and 15% c-PEQDA-PEI 330-2h is 38.7%, 83.4% and 89.9%, respectively.

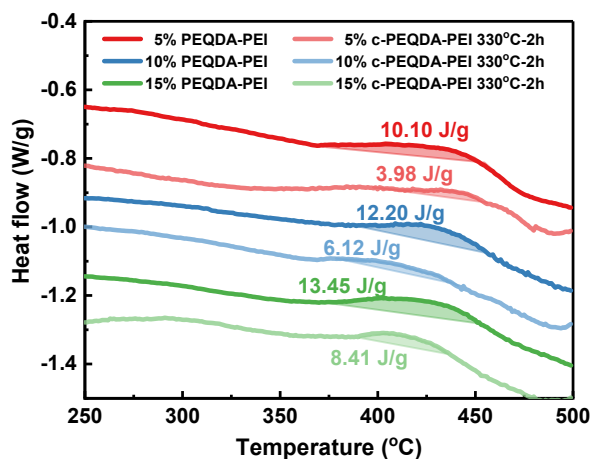


Figure S5. DSC profiles of PEQDA-PEI and c-PEQDA-PEI films.

The enthalpy of heat release of phenylethynyl crosslinking of the crosslinking films were characterized by DSC. As shown in Figure S5, the exothermic peak of the phenylethynyl crosslinking reaction appears at 400 °C. As the PEQDA content increases, the enthalpy of heat release gradually increases.

Table S2. Phenylethynyl crosslinking content of c-PEQDA-PEI films.

Crosslinking film	Crosslinking program	Crosslinking density (%)
5% c-PEQDA-PEI	330°C-2h	3.03
10% c-PEQDA-PEI	330°C-2h	4.98
15% c- PEQDA -PEI	330°C-2h	5.62

To intuitively know the proportion of crosslinking in the dianhydride, the content of phenylethynyl crosslinking in dianhydride is statistically analyzed in table S2. Under the same heat treatment process, the higher the content of crosslinkable dianhydride

PEQDA, the content of phenylethynyl crosslinking exhibits an upward trend until it nears $x\%/2$, which is consistent with the trend of increasing gel content. The phenylethynyl crosslinking contents of 5%, 10% and 15% c-PEQDA-PEI 330-2h are 3.03%, 4.98% and 5.62%, respectively. When PEQDA content is 15%, although the gel content reaches about 90%, only about 40% of the phenylethynyl group in the film react for crosslinking.

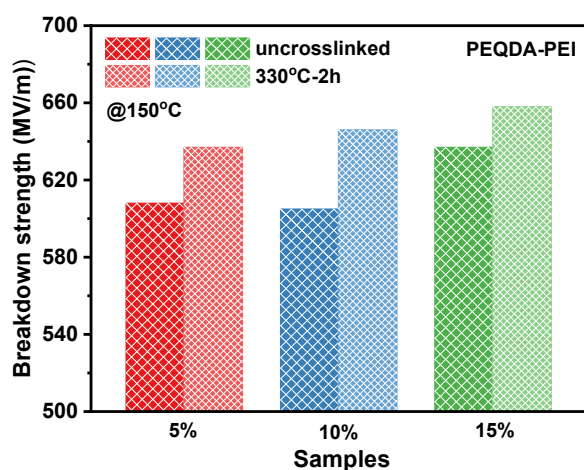


Figure S6. the summarized breakdown strength for films with different contents of PEQDA before and after crosslinking.

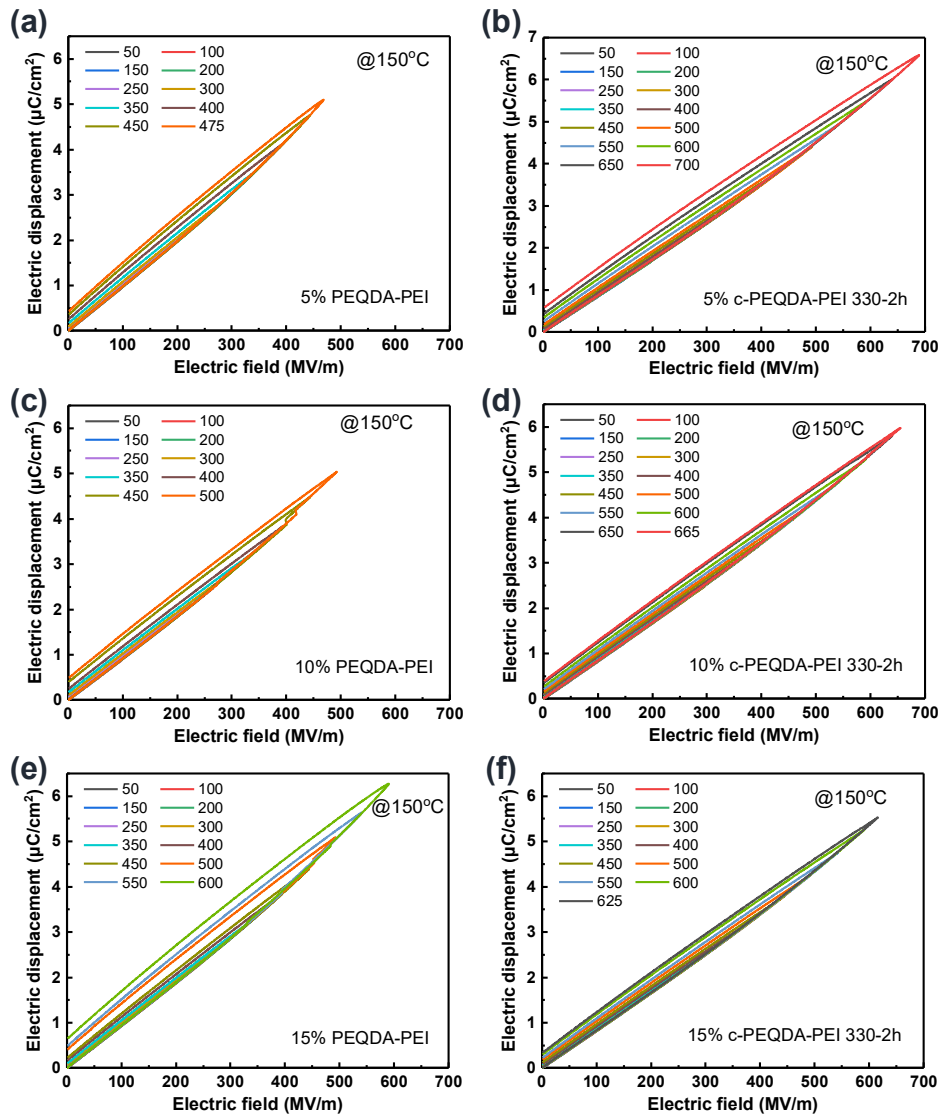


Figure S7. $P-E$ loops of PEQDA-PEI and c-PEQDA-PEI films at $150\text{ }^{\circ}\text{C}$.

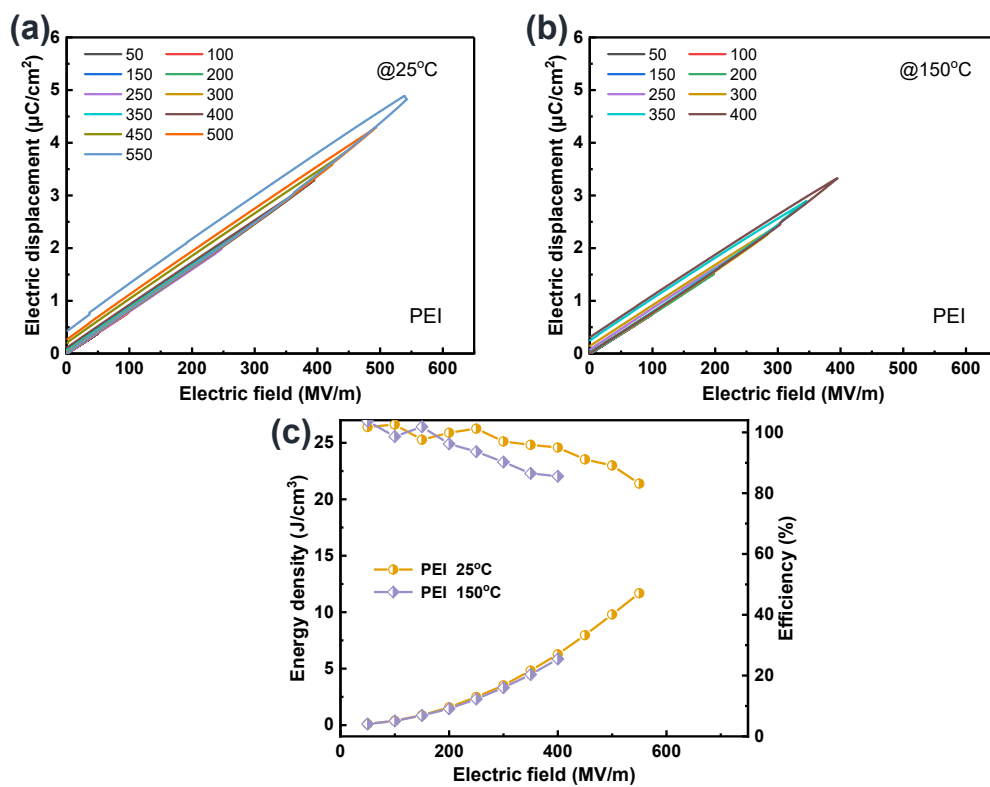


Figure S8. The energy storage capability of PEI film: (a) *P-E* loops at 25 °C, (b) *P-E* loops at 150 °C, and (c) discharged energy density and charge–discharge efficiency.

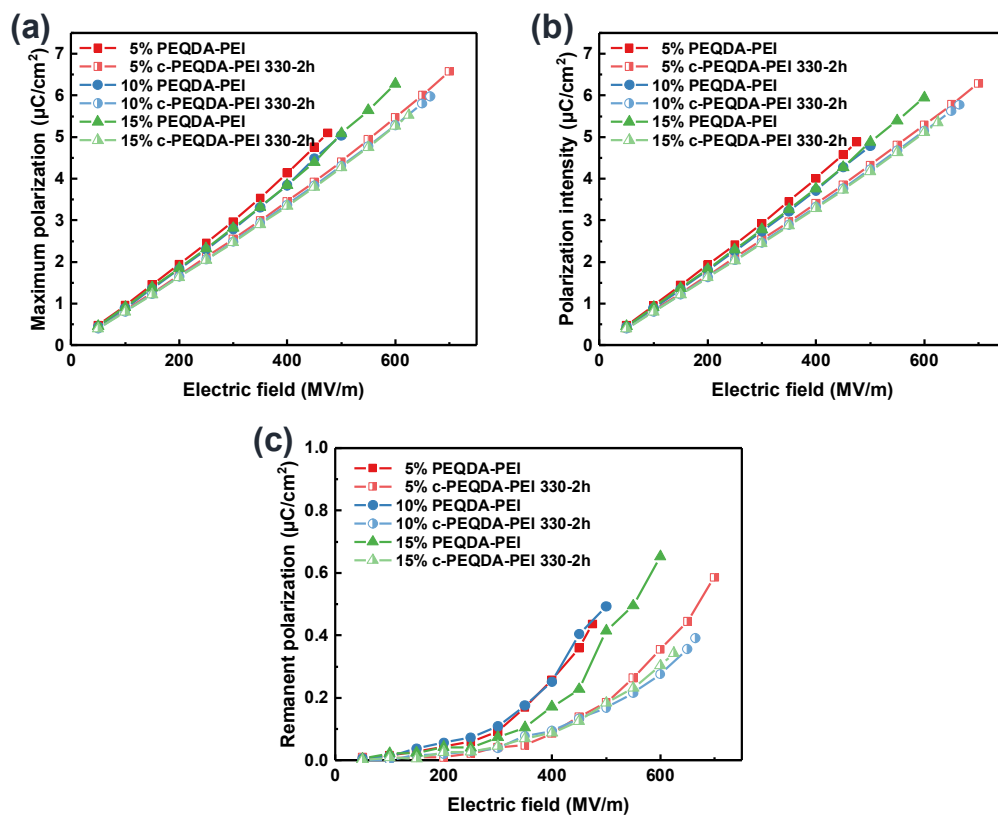


Figure S9. The polarizations of c-PEQDA-PEI films at 150 °C: (a) maximum polarization, (b) remnant polarization, and (c) net polarization.

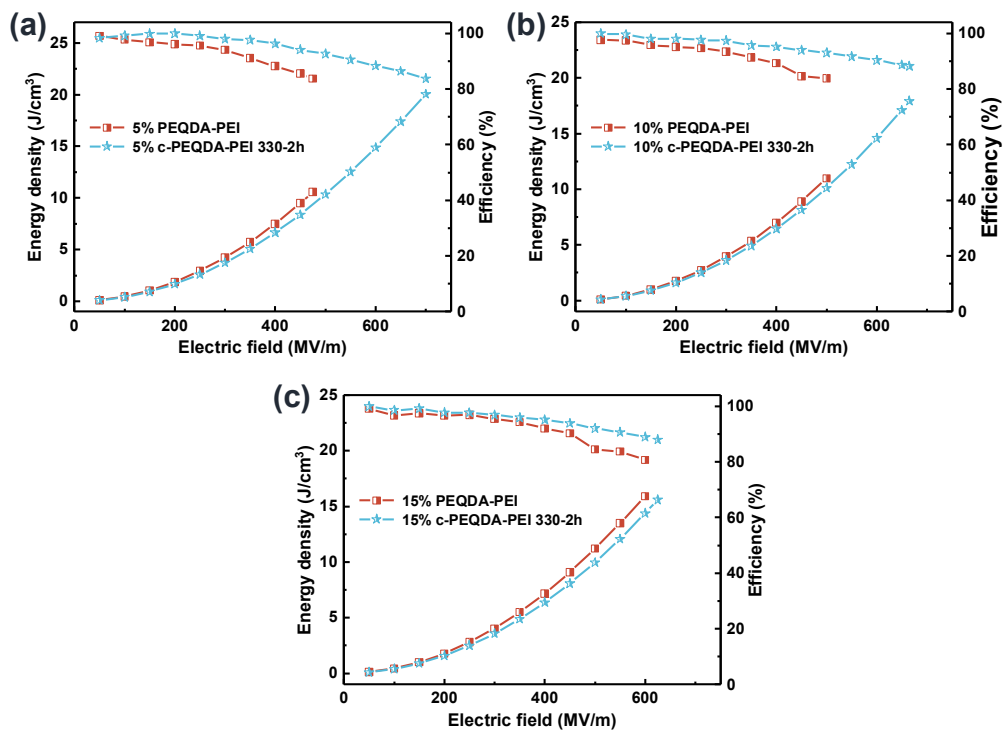


Figure S10. Discharged energy density and charge–discharge efficiency at 150 °C for c-PEQDA-PEI with different PEQDA contents: (a) 5%, (b) 10%, and (c) 15%.

Table S3. Average interchain spacing of c-PEQDA-PEI films.

Crosslinking film	Amorphous scattering peak (2θ)	Average interchain spacing (\AA)
5% PEQDA-PEI	17.66	5.023
5% c- PEQDA-PEI 330°C-2h	17.30	5.126
10% c- PEQDA-PEI 330°C-2h	18.26	4.859
15% c- PEQDA-PEI 330°C-2h	17.78	4.989

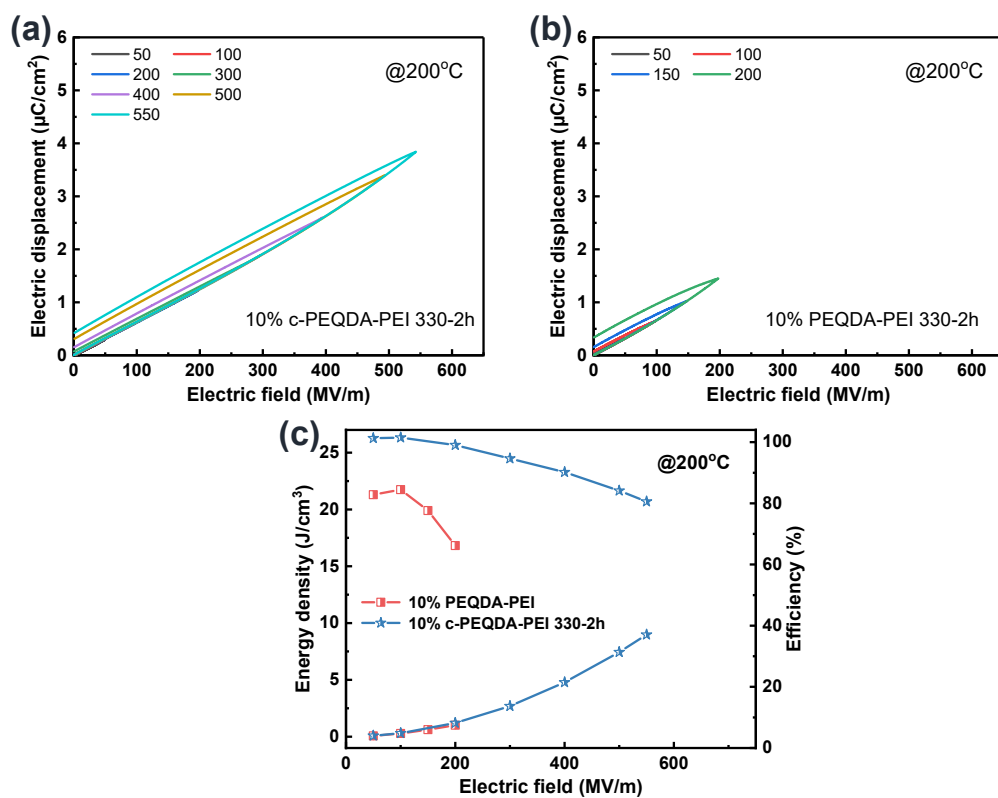


Figure S11. The energy storage capability of 10% c-PEQDA-PEI film: (a) $P-E$ loops of 10% c-PEQDA-PEI, (b) $P-E$ loops of 10% PEQDA-PEI film, and (c) discharged energy density and charge–discharge efficiency. The testing environmental temperature is 200 °C.